2019-11-25

Ocean community warming responses explained by thermal affinities and temperature gradients

Burrows, MT

10.1038/s41558-019-0631-5
Nature Climate Change
Springer Science and Business Media LLC

Ocean community warming responses explained by thermal affinities and temperature gradients

Michael T. Burrows[1*], Amanda E. Bates[2,3], Mark J. Costello[4], Martin Edwards[5,6], Graham J. Edgar[7], Clive J. Fox[1], Benjamin S. Halpern[8,9,10], Jan G. Hiddink[11], Malin L. Pinsky[12], Ryan D. Batt[12], Jorge García Molinos[13,14], Benjamin L. Payne[1], David Schoeman[15,16], Rick D. Stuart-Smith[7], Elvira S. Poloczanska[17,18]

As ocean temperatures rise, species distributions are tracking towards historically cooler regions in line with their thermal affinity[1, 2]. However, different responses of species to warming and changed species interactions makes predicting biodiversity redistribution and relative abundance a challenge[3, 4]. Here we use three decades of fish and plankton survey data to assess how warming changes the relative dominance of warm-affinity and cold-affinity species[5, 6]. Regions with stable temperatures show little change in dominance structure (Northeast Pacific, Gulf of Mexico), while warming sees strong shifts towards warm-water species dominance (North Atlantic). Importantly, communities whose species pools had diverse thermal affinities and narrower range of thermal tolerance show greater sensitivity, as anticipated from simulations. Composition of fish communities changed less than expected in regions with strong temperature depth gradients. There, species track temperatures by moving deeper[2, 7], rather than horizontally, analogous to elevation shifts in land plants[8]. Temperature thus emerges as a fundamental driver for change in marine systems, with predictable restructuring of communities in the most rapidly warming areas using metrics based on species thermal affinities. The ready and predictable dominance shifts suggests a strong prognosis of resilience to climate change for these communities.

Abundance and distributions of marine species are changing in response to anthropogenic climate change[1] but these changes vary geographically and across taxa. Shifts in geographical range and temporal species turnover, for example, tend to be accelerated where temperature changes coincide with widely spaced isotherms[1, 2]. Unlike terrestrial ecosystems, marine species may be unable to shelter

from extreme temperatures, making the effect of ambient temperature immediate, unavoidable, and easier to detect. Local gain and loss of species, combined with changes in the relative abundance of species with different thermal affinities, drive change in community structure. On land, failure of species distributions to track temperature means that community thermal composition lags behind expected change, seen in communities of birds, butterflies, and plant species [5, 9, 10, 11, 12, 13, 14]. Identifying the aspects of community change that can be accurately forecasted is needed to assist managers to adaptively deal with ecosystem change.

We use time series of species incidence in standardised international surveys of plankton and demersal (seabed-living) species since 1985 (Supplementary Table 1) to quantify regional changes in community structure. Combined with estimates of species' thermal affinities, these data describe regional changes in the average thermal affinity of marine communities, as measured by the Community Temperature Index (CTI, Supplementary Table 2). CTI is the community-wide average of species' thermal affinities, which are calculated from each Species Temperature Index, STI (the median of sea surface temperatures across each species' estimated geographical range, see Methods and Fig. 1a). The variation of thermal affinities among species (Community Thermal Diversity, CTDiv) is here described by the incidence-weighted standard deviation of STIs. Low values of thermal diversity reflect communities composed of species with similar STIs, and high values reflect communities composed of a mix of warm- and cold-water species. The incidence-weighted average width of species' thermal ranges (STRs, Fig. 1a), the Community Thermal Range (CTR), indicates whether communities are composed of broad-ranged species (eurytherms) or narrow-ranged species (stenotherms). The fact that distributions of marine ectotherms generally fill their thermal tolerances[15] supports the inference that thermal range can be approximated by species' geographic range.

The difference between CTI and local temperature (used to define STIs) is termed community thermal bias: positive where communities are dominated by species from warmer areas, implying reduced sensitivity to warming[16], and negative for communities dominated by species from colder areas, implying increased vulnerability[17]. Less compositional change in response to temperature is expected in areas of strong vertical and horizontal gradients in ocean temperature (and low velocity of climate change[18]) because small shifts may allow species to remain in the same temperature as before. Thermal bias is distinct from CTI lag[5] or extinction debt, since it refers to the difference in spatial patterns of temperature and average thermal affinity rather than to a perceived delay in community response to temperature change.

We focused on the sensitivity of CTI to regional temperature change (sCTI), defined as the ratio of the change in CTI through time to the corresponding change in environmental temperature. We evaluated the influence of community thermal diversity and community thermal range on CTI sensitivity by developing quantitative expectations from simulations. These simulated communities comprised pools of species with a thermal diversity set by the standard deviation of STI values. Each species had incidence-temperature curves[19] defined by their thermal range (Gaussian Fig. 1a, other forms in Supplementary Fig. 1), consistent with organisms more abundant near the middle of their range[20, 21]. While contested[22], the Gaussian pattern holds for our fish and plankton datasets (Fig. 1b, Supplementary Fig. 3) when abundance and incidence data are expressed relative to thermal range location. We used species' thermal ranges and temperature changes to simulate changes in species incidence with temperature which, when aggregated across species, produced changes in CTI. Simulated CTI sensitivity was large where thermally diverse communities were made up of narrow-ranged species[17] (Fig. 1c, g), but smaller where thermal ranges were broad or thermal diversity was low (Fig. 1d, f, g). For functions with declining abundance from a central maximum, simulated CTI sensitivity suggested more change in thermally diverse communities made up of small-ranged species,

and less in communities of species with similar thermal affinities and large thermal ranges (Supplementary Fig. 2, Supplementary Table 4). With Gaussian curves, CTI sensitivity was proportional to the squared ratio of thermal diversity to average range width (Fig 1g and Supplementary Table 2), independent of thermal bias. Below we explored this hypothesized relationship with empirical data.

Spatial patterns in CTI for demersal species and plankton, averaged from 1985 to 2014, broadly followed patterns in surface temperatures in the HadISST1 dataset[23] and seabed temperatures from the Hadley Centre EN4 dataset[24] (Supplementary Figs. 5a, 9a). Community thermal diversity was highest midway along thermal gradients. Thermal ranges were larger for plankton than demersal species, with plankton thermal ranges increasing in size with latitude (Supplementary Figs. 5b, 6). Average species' thermal affinity and range width in 2° grid cells were positively correlated in cool-temperate latitudes, where cold-affinity species having smaller thermal ranges than those from lower latitudes, and negatively correlated towards sub-tropical areas (Supplementary Fig. 6d). This pattern results from the bounds on species thermal ranges at the equator and the poles (Supplementary Figs 5, 6).

For SST-derived CTIs, areas with strong vertical temperature gradients had more negative community thermal bias in demersal species (Fig. 3a), with species' STIs more associated with cooler subsurface (50-100 m) rather than surface temperature. Plankton community thermal bias was less influenced by vertical gradients, suggesting a stronger association with surface temperatures. CTI derived from seabed temperature was more weakly associated with the spatial pattern in SBT (Methods, Supplementary Fig. 9g).

Both plankton and demersal communities, aggregated over 2° areas, changed in thermal affinity from 1985 to 2014 (Fig. 2, Supplementary Fig. 8) at local (<500 km) to ocean-basin scales (10,000 km). Sea surface temperatures warmed across the North Atlantic over this period by up to 0.5°C per

97 decade, but cooled slightly or stayed the same in the Northeast Pacific (Fig. 2a,b). Regional trends in
98 CTI for plankton and for demersal fish and invertebrates more clearly followed trends in sea surface
99 temperature ($R^2 = 0.23$, Fig. 2e) than seabed temperature ($R^2 = 0.1$ Supplementary Fig. 9g). Demersal
100 communities shifted towards dominance by warm-water species around northeast USA and Europe,
101 while North Pacific, southeast USA and other areas with little temperature change had stable CTIs (Fig.
102 2c). CTI changes in plankton communities were also most pronounced in areas of greater SST change
103 in the northwest Atlantic and the northwest European Shelf (Fig. 2d).

104 In European waters, CTI for demersal species changed more consistently than plankton CTI (Fig.
105 2c,d), especially in the southern North Sea, despite observed large distribution changes in plankton
106 species[25]. Reduced CTI sensitivity in plankton is expected given the greater temperature ranges of
107 plankton species compared to demersal invertebrates and fishes (Supplementary Figs 5c, 6d). The
108 positive effect of thermal diversity and inverse effect of community thermal range (CTR) on CTI
109 sensitivity explained much of the variability in responses of community composition to warming
110 (R^2=0.39), but the negative and near-zero response of Canadian demersal communities remained (Fig.
111 3c). Vertical gradients in temperature (up to 7°C over the top 50m) explained much of the remaining
112 variation in sensitivity of CTI to temperature, improving the performance of regression models (Fig.
113 3c, Supplementary Table 4). SST-derived thermal bias in natural communities had a small positive
114 effect on sensitivity, but this effect was lost when compared alongside vertical and horizontal gradients
115 in regression models (Supplementary Table 4, Model R1). Horizontal spatial gradients in surface
116 temperature had no effect on CTI sensitivity when considered with vertical gradients (Supplementary
117 Table 4).

118 Reduced CTI sensitivity to surface warming in areas of steep vertical temperature gradients is
119 consistent with a redistribution of species to greater depths[26]. Such vertical gradients may allow

120 thermal niche tracking without horizontal shifts, and may provide refugia for cold-water species
121 without significant ecological consequences, unless limited to the surface by a need for light
122 (phytoplankton, coral, macroalgae), or habitat (intertidal organisms). The lack of influence of
123 horizontal thermal gradients on CTI sensitivity to surface temperature change suggests that horizontal
124 shifts in species distribution had comparatively little effect at the scale of the analysis (2° × 2° grids
125 over 30 years).

126 Patterns of observed CTI sensitivity matched expectations from simulations. More change in
127 community composition was seen in communities composed of species with greater diversity of
128 thermal affinities, narrower thermal ranges, and without access to refuges from climate change at
129 greater depths (i.e., outside areas of steep vertical temperature gradients where observed changes do not
130 match predictions). While negative thermal bias has been implicated as an indicator for community-
131 level vulnerability with warming[17], we found instead instances of apparent negative SST-derived
132 thermal bias (e.g. demersal species in the Canadian Atlantic Maritimes: Fig. 3a) that were better
133 explained by vertical temperature gradients, with species' affinities closer to temperatures experienced
134 at depth than surface temperatures.

135 Studies of birds, butterflies and plant communities showing smaller changes in CTI than changes
136 in temperature have generally been interpreted as lags in response[5, 9, 10, 11, 12], but thermal range width
137 and community thermal range effects on CTI sensitivity may explain some of these apparent lags.
138 Short-lived plankton and species of highly mobile fish and invertebrates may be more responsive to
139 temperature change in time and space[2, 6] than analogous communities on land, potentially as a
140 consequence of living closer to their thermal limits[27]. Communities of long-lived, slowly dispersing
141 species may be less responsive in thermal affinity composition when increasing in abundance, but may
142 decline rapidly, as in the loss of cold-water kelp and influx of tropical fish in response to a recent

143 warming event in Western Australia[28]. Slower-than-expected community responses may also be caused
144 by compensatory population dynamics[29] in individual species. Replacement of cooler-affinity species
145 by incoming warmer-affinity species is not possible in the tropics, likely resulting in the depression in
146 species richness at the equator[30]. In addition, geographical barriers can also restrict routes for incoming
147 migrants, such as in the Mediterranean[31], resulting in a lowered species turnover[6] and capacity for CTI
148 change[17].

149 Our study shows the dominant effects of recent temperature change on community turnover across
150 marine species from regional to ocean scales, regardless of other influences such as fishing impacts and
151 ocean acidification. The prediction of temperature effects at community scales derived from species
152 thermal performance curves[32] provides a benchmark against which the pace of reorganization of global
153 biodiversity to climate can be judged, and allows assessment of the performance of quantitative
154 models[3, 4]. The predictability with which thermal diversity, average thermal range width and vertical
155 temperature gradients directly drive patterns of sensitivity of community composition to warming gives
156 a strong prognosis for the resilience of ocean communities to respond to climate change. In the
157 northern temperate coastal oceans in this study, warm-tolerant species of plankton and fishes are slowly
158 replacing their cold-tolerant counterparts over the timescales of climate change, and if those species
159 have similar roles, suggesting a capacity for the oceans to continue to function.

160 **Methods**

161 Methods, including statements of data availability and any associated accession codes and
162 references, are available in the online version of this paper.

163 **References**

164 1. Poloczanska ES, Brown CJ, Sydeman WJ, Kiessling W, Schoeman DS, Moore PJ*, et al.* Global
165 imprint of climate change on marine life. *Nature Climate Change* 2013, **3:** 919-925.
166 2. Pinsky ML, Worm B, Fogarty MJ, Sarmiento JL, Levin SA. Marine taxa track local climate
167 velocities. *Science* 2013, **341**(6151)**:** 1239-1242.

3. Jones MC, Cheung WWL. Multi-model ensemble projections of climate change effects on global marine biodiversity. *ICES Journal of Marine Science: Journal du Conseil* 2015, **72**(3)**:** 741-752.
4. García Molinos J, Halpern BS, Schoeman DS, Brown CJ, Kiessling W, Moore PJ*, et al.* Climate velocity and the future global redistribution of marine biodiversity. *Nature Climate Change* 2016, **6**(1)**:** 83.
5. Devictor V, van Swaay C, Brereton T, Brotons Ls, Chamberlain D, Heliölä J*, et al.* Differences in the climatic debts of birds and butterflies at a continental scale. *Nature Climate Change* 2012, **2**(2)**:** 121.
6. Cheung WWL, Watson R, Pauly D. Signature of ocean warming in global fisheries catch. *Nature* 2013, **497**(7449)**:** 365-368.
7. Perry AL, Low PJ, Ellis JR, Reynolds JD. Climate change and distribution shifts in marine fishes. *Science* 2005, **308**(5730)**:** 1912-1912.
8. Lenoir J, Gégout JC, Marquet PA, de Ruffray P, Brisse H. A significant upward shift in plant species optimum elevation during the 20th century. *Science* 2008, **320**(5884)**:** 1768.
9. Lindström Å, Green M, Paulson G, Smith HG, Devictor V. Rapid changes in bird community composition at multiple temporal and spatial scales in response to recent climate change. *Ecography* 2013, **36**(3)**:** 313.
10. Nieto-Sánchez S, Gutiérrez D, Wilson RJ. Long-term change and spatial variation in butterfly communities over an elevational gradient: driven by climate, buffered by habitat. *Divers Distrib* 2015, **21**(8)**:** 950.
11. Santangeli A, Rajasärkkä A, Lehikoinen A. Effects of high latitude protected areas on bird communities under rapid climate change. *Glob Change Biol* 2017, **23**(6)**:** 2241-2249.
12. Bertrand R, Lenoir J, Piedallu C, Riofrío-Dillon G, de Ruffray P, Vidal C*, et al.* Changes in plant community composition lag behind climate warming in lowland forests. *Nature* 2011, **479**(7374)**:** 517.
13. De Frenne P, Rodríguez-Sánchez F, Coomes DA, Baeten L, Verstraeten G, Vellend M*, et al.* Microclimate moderates plant responses to macroclimate warming. *Proceedings of the National Academy of Sciences* 2013, **110**(46)**:** 18561-18565.
14. Flanagan PH, Jensen OP, Morley JW, Pinsky ML. Response of marine communities to local temperature changes. *Ecography* 2018.
15. Sunday JM, Bates AE, Dulvy NK. Thermal tolerance and the global redistribution of animals. *Nature Climate Change* 2012, **2**(9)**:** 686-690.
16. Deutsch CA, Tewksbury JJ, Huey RB, Sheldon KS, Ghalambor CK, Haak DC*, et al.* Impacts of climate warming on terrestrial ectotherms across latitude. *Proceedings of the National Academy of Sciences* 2008, **105**(18)**:** 6668-6668.
17. Stuart-Smith RD, Edgar GJ, Barrett NS, Kininmonth SJ, Bates AE. Thermal biases and vulnerability to warming in the world's marine fauna. *Nature* 2015, **528**(7580)**:** 88-92.
18. Burrows MT, Schoeman DS, Buckley LB, Moore P, Poloczanska ES, Brander KM*, et al.* The pace of shifting climate in marine and terrestrial ecosystems. *Science* 2011, **334**(6056)**:** 652-655.
19. Beaugrand G. Theoretical basis for predicting climate-induced abrupt shifts in the oceans. *Philosophical Transactions of the Royal Society B: Biological Sciences* 2015, **370**(1659)**:** 20130264.
20. Brown JH. On the relationship between abundance and distribution of species. *Am Nat* 1984, **124**(2)**:** 255–279.
21. Waldock C, Stuart‐Smith RD, Edgar GJ, Bird TJ, Bates AE. The shape of abundance distributions across temperature gradients in reef fishes. *Ecol Lett* 2019, **22**(4)**:** 685-696.

22. Sagarin RD, Gaines SD. The 'abundant centre' distribution: to what extent is it a biogeographical rule? *Ecol Lett* 2002, **5**(1)**:** 137-147.
23. Rayner NA, Parker DE, Horton EB, Folland CK, Alexander LV, Rowell DP*, et al.* Global analyses of sea surface temperature, sea ice, and night marine air temperature since the late nineteenth century. *J Geophys Res* 2003, **108**(D14)**:** 4407-4407.
24. Good SA, Martin MJ, Rayner NA. EN4: Quality controlled ocean temperature and salinity profiles and monthly objective analyses with uncertainty estimates. *Journal of Geophysical Research: Oceans* 2013, **118**(12)**:** 6704-6716.
25. Beaugrand G, Luczak C, Edwards M. Rapid biogeographical plankton shifts in the North Atlantic Ocean. *Glob Change Biol* 2009, **15:** 1790-1803.
26. Dulvy NK, Rogers SI, Jennings S, Stelzenmüller V, Dye SR, Skjoldal HR. Climate change and deepening of the North Sea fish assemblage: a biotic indicator of warming seas. *J Appl Ecol* 2008, **45**(4)**:** 1029–1039-1029–1039.
27. Pinsky ML, Eikeset AM, McCauley DJ, Payne JL, Sunday JM. Greater vulnerability to warming of marine versus terrestrial ectotherms. *Nature* 2019, **569**(7754)**:** 108.
28. Wernberg T, Smale DA, Tuya F, Thomsen MS, Langlois TJ, de Bettignies T*, et al.* An extreme climatic event alters marine ecosystem structure in a global biodiversity hotspot. *Nature Climate Change* 2013, **3:** 78-82.
29. Doak DF, Morris WF. Demographic compensation and tipping points in climate-induced range shifts. *Nature* 2010, **467**(7318)**:** 959.
30. Chaudhary C, Saeedi H, Costello MJ. Bimodality of latitudinal gradients in marine species richness. *Trends Ecol Evol* 2016, **31**(9)**:** 670-676.
31. Burrows MT, Schoeman DS, Richardson AJ, Molinos JG, Hoffmann A, Buckley LB*, et al.* Geographical limits to species-range shifts are suggested by climate velocity. *Nature* 2014, **507**(7493)**:** 492.
32. Pörtner HO, Farrell AP. Physiology and climate change. *Science* 2008, **322**(5902)**:** 690.

Supplementary Information is linked to the online version of the paper at www.nature.com/nature.

Acknowledgements

M.T.B., B.P., J.G.M. were supported by NERC grant NE/J024082/1; J.G.M. by the “Tenure-Track System Promotion Program" of the Japanese Ministry of Education, Culture, Sports, Science and Technology; D.S.S., G.J.E and R.D.S-S by the Australian Research Council grants DP170101722, LP150100761 and DP170104240, respectively; M.L.P. by National Science Foundation grants OCE-1426891 and DEB-1616821, an Alfred P. Sloan Research Fellowship, and the NOAA Coastal and Ocean Climate Applications program; and A.E.B. by the Canada Research Chairs Program. Data sources used here are listed in Supplementary Materials.

Author contributions

M.T.B., A.E.B., M.L.P., R.S.-S. and E.S.P. conceived the research. M.T.B. and B.P. analysed the data. M.T.B., A.E.B, B.P, J.G.M. wrote the first draft. All authors contributed equally to discussion of ideas and analyses, and commented on the manuscript.

Author information

The authors declare no competing financial interests. Correspondence and requests for materials should be addressed to M.T.B. (mtb@sams.ac.uk).

Affiliations

[1*]Scottish Association for Marine Science, Scottish Marine Institute, Dunbeg, Oban, Argyll, PA37 1QA. [2]Ocean and Earth Sciences, National Oceanography Centre Southampton, University of Southampton Waterfront Campus, Southampton SO14 3ZH, UK. [3]Department of Ocean Sciences, Memorial University of Newfoundland, St. John's A1C 5S7, Canada. [4]School of Environment, University of Auckland, Auckland, New Zealand 1142. [5]Sir Alister Hardy Foundation for Ocean Science, The Laboratory, Citadel Hill, Plymouth PL1 2PB, UK. [6]Marine Institute, Plymouth University, Plymouth, PL4 8AA, UK [7]Institute for Marine and Antarctic Studies, University of Tasmania, Hobart, Tasmania, 7001 Australia. [8]Bren School of Environmental Science & Management, University of California Santa Barbara, CA 93106-5131, USA. [9]National Center for Ecological Analysis & Synthesis, University of California, Santa Barbara, CA 93101, [11]School of Ocean Sciences Bangor University, Menai Bridge, Anglesey, LL59 5AB, UK. [12]Department of Ecology, Evolution, and Natural Resources, Rutgers University, 14 College Farm Rd., New Brunswick, NJ 08901, USA. [13]Arctic Research Center, Hokkaido University, N21W11 Sapporo, Hokkaido 001-0021, Japan. [14]Graduate School of Environmental Science, Hokkaido University, N10W5 Sapporo, Hokkaido 060-0810, Japan, [15]School of Science and Engineering, University of the Sunshine Coast, Maroochydore,

Queensland 4558, Australia. [16]Centre for African Conservation Ecology, Department of Zoology, Nelson Mandela University, Port Elizabeth, South Africa. [17]Alfred Wegener Institute, Helmholtz Centre for Polar and Marine Research, Division Biosciences/Integrative Ecophysiology, Am Handelshafen 12, 27570 Bremerhaven, Germany. [18]Global Change Institute, The University of Queensland, St Lucia, Queensland, Australia.

*e-mail: mtb@sams.ac.uk.

Figures

Fig. 1 | Simulated communities to illustrate the effects of thermal diversity and thermal range width on the sensitivity of Community Temperature Index (CTI) to temperature change. **a**, a Gaussian abundance-temperature distribution for Species Temperature Index (STI) = 15 and Species Thermal Range (STR) = 10. **b**, quantiles (a50 = 50th percentile etc.) of abundance across thermal ranges for US trawl survey species. **c-f**, Thermal characteristics in simulated pools of species varying in thermal diversity and thermal range, showing subsets forming communities at 15^{o}C mean annual sea temperature. **g**, Sensitivity in simulated communities (symbols) of Community Temperature Index (sCTI, the ratio of CTI change to temperature change) to changing Community Thermal Diversity (CTDiv). Thermal diversity in the species pool (standard deviation of STIs) and the species thermal range were changed for each simulated community of 1000 species, with average sCTIs shown for 1000 repeat runs. Grey lines and similar coloured symbols link simulated communities with the same thermal diversity, black lines linking communities with similar thermal ranges . Letters in **g** indicate the sensitivity of CTI associated with thermal diversity and thermal ranges in the example communities shown in **c-f**.

Fig. 2 | Trends in temperature and composition of demersal and plankton communities shown by Community Temperature Index (CTI_{SST}) values from 1985 to 2014. **a**, Trend in sea surface temperature (SST) from the Hadley Centre Sea Ice and Sea Surface Temperature data set (HadISST v1) where blue is colder and red warmer. **b**, as (**a**) aggregated into the 2° × 2° latitude-longitude grid cells surveyed for plankton and demersal fish. **c**, Trends in CTI_{SST} for bottom trawls, and **d**, for Continuous Plankton Recorder hauls. **e**, CTI_{SST} trends compared with SST trends. CTI trends are shown as bootstrap averages and standard deviations of computed regression slopes over time (n=500 using random selection of species with replacement). SST trends are shown as regression slopes ± standard errors. Symbol sizes are scaled by the number of years sampled, while colours denote the survey programme (black, CPR, Continuous Plankton Recorder; red, DFO, Department of Fisheries and Oceans, Canada; green, IBTS, International Bottom Trawl Survey; blue, NMFS, US National Marine Fisheries Service). The dependence of CTI_{SST} trend on SST trends per gridcell is shown by two regression slopes ± 95% confidence intervals: with an intercept term (solid line with grey shading, Model A, R^2=0.08) and without (line with red shading, Model B, R^2=0.23, Supplementary Table 4).

Fig. 3 | Trends in Community Temperature Index (CTI_{SST}) for Northern Hemisphere demersal and plankton communities from 1985 to 2014 influenced by near-surface vertical and horizontal temperature gradients. a, Thermal bias (CTI_{SST} –SST) versus vertical temperature gradient (lower regression through demersal species, upper regression through plankton). **b**, Difference between observed CTI trends and those predicted from surface temperature trends (Model B residuals) versus local Community Thermal Diversity. **c**, Residuals from a regression including SST trends combined with community thermal diversity, community thermal range (Model I residuals, mapped in **d**) versus local vertical temperature difference. Error bars in **a-c** show bootstrap standard errors for CTI_{SST} trend estimates. **e**, Vertical temperature gradients (0-50m, 1985-2014 from Hadley Centre EN4 dataset). **f**, Relationships among CTI sensitivity, vertical and horizontal temperature gradients and thermal bias shown by correlation (grey arrows, round parentheses) and regression beta coefficients (black arrows, square parentheses) from regression of residuals from **b** (Supplementary Table 4 Model R1).

Online only Methods

Simulation of sensitivity of the community temperature index to temperature change.

Expected effects on the response of community thermal indices to temperature change were explored in a simulation model based on species-level functions relating abundance to temperature. Four functional forms were used: (i) Gaussian, with abundance declining symmetrically away from a central optimum, (ii) a trimmed Gaussian, with a central plateau, and (iii) left- and right-skewed functions based on the gamma distribution (Supplementary Fig. 1). Pools of 1000 species were created by randomly selecting species' thermal midpoints (STI) from a Gaussian distribution with a mean of 15°C plus or minus an offset representing thermal bias [17], the degree to which the community is composed of types from warmer or colder conditions. Variation in thermal affinities in the species pool was manipulated via the standard deviation of STI values in the species pool, (sdSTI, species pool thermal diversity in Fig. 1e). Each species in the pool was assigned a thermal range (STR, species pool thermal range in Fig. 1e), as the difference between the 90th and 10th percentiles of the abundance-temperature function.

The four abundance-temperature functions (Supplementary Fig. 1) simulated different patterns of abundance across species ranges. The Gaussian function represented species that are more abundant, or occur in a greater proportion of samples, at the centre of the distribution range. In this form, the equivalent standard deviation for a given STR (the difference between the 10^{th} and 90^{th} percentiles of the distribution) was obtained by dividing STR by $2 \cdot t_{0.1,\infty}$ (the number of multiples of SD percentiles of a Gaussian distribution). Simulated abundance (or incidence) of any species across the range of temperatures considered, here 0°C to 30°C, was obtained from the probability density function of the Gaussian distribution with the species' STI as the mean and SD-equivalent range width as its standard deviation (as in Fig 1a-d). For the trimmed Gaussian function, simulated abundance between mean–SD

and mean+SD was set at the probability density value for the mean-SD and otherwise followed the standard Gaussian formulation. For the skewed functions based on the gamma distribution, simulated abundance was produced using the gamma probability density function for varying shape values, and scale factors obtained by dividing the STR by the difference between the 90th and 10th percentiles of each gamma distribution for the applicable shape value and a scale factor of 1.

Simulated abundance/incidence values were used to calculate Community Temperature Index values (CTI, abundance-weighted average STI) and Community Thermal diversity (CTDiv, abundance-weighted standard deviations of STI values) at different temperatures. The sensitivity of CTI to temperature change (sCTI) was measured by calculating CTI for species at temperatures 0.1°C below and above 15°C, and dividing the difference in CTI values by 0.2°C to give the ratio of CTI change to temperature change.

We used linear regression analysis to analyse the response of CTI sensitivity (sCTI) to the distribution of species thermal properties in these simulated communities. For the Gaussian abundance-temperature function, CTI sensitivity exactly depended on the squared ratio of CTDiv to STR (Supplementary Table 3, Model Z), with thermal bias having no meaningful effect. Adding variable Species Thermal Ranges (Supplementary Table 3, Model Z1) reduced the sensitivity of CTI to temperature at low levels of thermal diversity, but the effect was relatively small (Supplementary Table 5). With a flattened response of abundance to temperature emulated by the trimmed Gaussian function, the negative effect of average species thermal range (CTR) was completely eliminated. Communities composed of narrow- or wide-ranged species for the same level of thermal diversity had the same CTI sensitivity (Supplementary Fig. 2b). This suggests that CTI metrics estimated from range information alone would not be sensitive to the average range width of the species involved for this functional form.

For the asymmetrical abundance-temperature functions represented by the gamma and reversed gamma functions (Supplementary Fig. 1), the effects of varying CTDiv, CTR and the shape of the function were similar in both cases (Models Z3 and Z4, Supplementary Fig. 2c, 2e) but the effects of thermal bias depended on the direction of the skew. For the right-skewed gamma distribution, CTI sensitivity to temperature increased with thermal bias, producing a CTI that would change more rapidly with temperature if composed of warmer-water species. The left-skewed reverse gamma abundance-temperature function, with a shape more similar to physiological temperature performance curves, showed the opposite effect, with more sensitivity of CTI to temperature if the community was composed largely of species from colder waters. This behaviour suggests the rapid changes in abundance at temperatures above the optimum produce more rapid shifts in CTI than the more gradual changes in abundance below the optimum (Supplementary Fig. 1d). Notwithstanding such effects of functional form of the abundance-temperature response on the sensitivity of CTI to temperature, the observed patterns of abundance more closely followed the simple Gaussian function (see section: **Average abundance and incidence across species thermal ranges**).

Marine community data sources.

Five marine community datasets were used (Supplementary Table 1). For analysis of patterns in responses across spatially extensive time-series data, data from three bottom-trawl survey programs and one plankton sampling program were downloaded and prepared such that every taxon record in each sample (either a single trawl or section of Continuous Plankton Recorder silk) was associated with a latitude, longitude and date. The three bottom-trawl surveys were organized into different regional sampling programs, and data from each regional program were combined. US National Marine Fisheries Service (NMFS) data were obtained from the Ocean Adapt website and pre-processed using existing R code (Pinsky group, https://github.com/pinskylab/OceanAdapt downloaded February 2016).

393 European International Bottom Trawl Survey (IBTS) datasets were downloaded in a common format
394 with details of sizes of species caught and of each trawl, of which only the abundance, date and
395 location were used. Canadian Department of Fisheries and Oceans data came from the Ocean
396 Biogeographical Information System (OBIS) web portal, with similar details of sampling. Continuous
397 Plankton Recorder data were obtained directly from the Continuous Plankton Recorder Survey,
398 including date of hauls, longitude and latitude alongside estimated species abundance.

399 Each dataset recorded abundance in a different way but, for every dataset including those that
400 lacked abundance data, analyses were possible using species incidence among samples taken in the
401 aggregating location and period. Species incidence (the relative frequency of trawls in which the
402 species occurred, for data aggregated by area and time period) was used as the weighting factor in all
403 calculations of community thermal metrics (CTI, CTDiv, CTR), and was highly correlated with
404 abundance when available (Supplementary Fig. 10).

405 **Ocean temperature data.**

406 We used five sea-surface-temperature datasets and one layered subsurface dataset for analysis of
407 temperature change in the study region (Supplementary Table 1). Annual sea surface temperatures per
408 1° latitude-longitude grid cell were averaged over 1985 to 2014 for each dataset to represent long-term
409 climate over the period of surveys. Seabed temperatures were derived from the deepest layer in the
410 Hadley Centre EN4 dataset and averaged over the same period. Trends in °C/yr were calculated for 1°
411 cells using annual means from 1985 to 2014 (Fig. 2e, Supplementary Fig. 13). Vertical gradients in
412 temperature (Fig. 3d) were calculated using the EN4 dataset[25] from layer means (surface: 5.02m,
413 “50m”: 45.4m, “100m”: 98.3m, “200m”: 207.4m) based on annual means from 1985 to 2014 .

Derivation of Species Temperature Indices (STIs) and fitted Maxent models.

Global predicted distribution maps were produced using presence-only Maxent models for each species in fish and plankton datasets occurring in ten or more 1° cells, and using default parameters for a random seed, convergence threshold, maximum number of iterations, maximum background points and the regularization parameter[3] (Maxent version 3.3.3k). Observations of species presence from OBIS were gridded such that 1° grid cells with observations were set as present. Only 2% of species were found in <10 1°latitude/longitude gridcells, with most species found in 10 to 100 gridcells (10-32, 36%; 32-100, 37%; >100, 24%). These observations were then modelled as a function of the following environmental predictors: (1) average annual temperatures from the HadISST v1.1; (2) the logarithm of distance to the nearest coastline; (3) ocean depth from the GEBCO marine atlas; and (4) FAO major fishing areas (http://www.fao.org/fishery/area/search/en). Frequency of all records in OBIS in 1° grid cells was used as the bias correction file. Although we did not additionally spatially thin the input records as has been suggested[33], the reduction of records to presence in 1° cells and inclusion of the bias file were attempts to reduce spatial bias due to uneven sampling effort. Global maps of predicted presence were produced using a threshold probability of 0.4, restricting the range of possible areas to those of high suitability[4].

Resulting Maxent-predicted distribution maps were used to extract sea temperature values from long-term climatology average 1985-2014 from HadISST (henceforth CTIhadsst1), EN4 surface (averaged across species to give CTIen4sst) and EN4 seabed (giving CTIen4sbt). Quantiles (0, 0.1, 0.25, 0.5, 0.75, 0.9 and 1.0, area-weighted by the cosine of the latitude) of these map-extracted temperatures were used to define the thermal niche of the species. The 50th percentile (median) of temperatures in occupied areas was used as the Species Temperature Index (STI, derived separately for HadISST and EN4 SST and seabed). The difference between 10th and 90th percentile temperatures (T_{90} – T_{10}, Fig. 1a) defined the Species Thermal Range (STR). A Species Temperature Index derived as the

438 average of T_{90} and T_{10} values obtained from species presence in 1° grid cells (giving CTIhadsst2 and
439 directly comparable to [17]) was also used to compare analyses based on observation-derived thermal
440 affinities with analyses derived from modelled distributions (CTIhadsst1).

441 Patterns in ocean temperature were used twice in the analysis: (i) as long-term mean values
442 matched to modelled species distributions to derive STIs and STRs, and (ii) as local trends over the 30-
443 year study period to compare with local trends in CTI values. Despite the use of information on sea
444 temperature more than once, information flows in the derivation of species thermal affinities and
445 analysis of spatial patterns were separate from those in the analysis of temporal patterns in community
446 thermal composition related to temperature trends (Supplementary Fig. 4). These separate pathways
447 allowed us to avoid circularity in reasoning.

448

449 **Average incidence (relative frequency of occurrence) across species thermal ranges.**

450 The form of the relationships of species incidence with range location was determined by first
451 matching species' incidence to local temperatures in 2° grid cells, and then locating those temperatures
452 relative to the thermal limits of the distribution of each species (Fig. 1b, Supplementary Fig. 3).
453 Average incidence values were calculated for every species in 2° latitude-longitude grid cells as the
454 frequency of samples in which the species occurred, expressed as a proportion of the total number of
455 samples across the whole period of each survey. Range location was derived from the average
456 temperature in the cell relative to range limits (Fig. 1b, T_{10} and T_{90}, equation in Supplementary Table
457 2).. Incidence values per 2° cell were rescaled for every species to give values relative to the average
458 incidence within the STR, so reducing the effect of prevalent species on the resulting pattern.
459 Percentiles (50%, 75%, 90%) of scaled-incidence values were then calculated in range-location unit
460 classes of 1/25 from -2 to 2 (Fig. 1b, Supplementary Fig. 3). To check how well incidence reflected

species abundance, calculations were repeated for abundance measures where available (average weight per trawl for NMFS data and number per haul for CPR and IBTS data) by summing numbers or biomass and dividing this sum by the total number of samples in each 2° latitude-longitude grid cell (Supplementary Fig. 3). Abundance changes across thermal ranges were calculated in the same way as incidence changes.

Community Temperature Index (CTI), Thermal Diversity (CTDiv), average Species Thermal Range (CTR) and Thermal Bias in surveys.

CTI values were calculated as incidence-weighted average STIs using data aggregated in 2° × 2° areas to produce maps (Supplementary Figures 4 and 9), and temporal trends (Fig. 2). Community thermal diversity, CTDiv, the spread of STI values around each CTI measure, was similarly calculated as the incidence-weighted standard deviation of the STIs for species present in the grid cell or grid cell/ year combination. Community thermal range (CTR) was the incidence-weighted average of species' STR values. Incidence (relative frequency of species in samples per aggregation unit) was used as the weighting factor because abundance was expressed differently in each dataset (Supplementary Table 1): as total numbers per trawl sample (IBTS data), biomass per haul (NMFS data), and as scores per silk (CPR data). However, incidence was strongly related to abundance in each set for which abundance data were available (Supplementary Fig. 8). Thermal bias was calculated as the CTI minus local sea temperature (using whichever temperature dataset was used to derive corresponding STIs), giving positive values where more species were from warmer areas and negative values where the species were from cooler places.

Uncertainty in CTI estimation is often poorly estimated[34] so, in addition to the four alternative methods of derivation of STIs, we used bootstrap resampling of species to generate standard errors and confidence intervals for means and trends in CTI and for the outcomes of more complex regression

484 analyses. Bootstrap sets of species were randomly selected with replacement from those in each survey
485 scheme (141 CPR, 285 IBTS, 585 NMFS, and 285 DFO species). The frequency of each species in the
486 bootstrap set was used as a multiplier on species incidence as the weighting factor (w_i in
487 Supplementary Table 2) to give bootstrap estimates of each of the community thermal metrics. Each
488 metric (annual mean, anomaly, trend) and regression model was computed for 500 repeated bootstrap
489 species selections, and summarised to give bootstrap averages, standard errors and 95% confidence
490 intervals.

491 For time-series analysis, the annual CTI values averaged per 2° × 2° grid cell were expressed as an
492 anomaly from the 1985-2014 average CTI for that cell. US NMFS data had several regional series that
493 occurred together in the same grid cell, notably in the Northeast and Southeast US spring and fall
494 series. In this case, anomalies were calculated for each series separately then averaged to give final CTI
495 values for that cell. Trends in CTI for each 2° × 2° cell were calculated using all years for which CTI
496 values were available, and matching trends for SST values were calculated for the same set of years.

497 **Uncertainty in annual CTI anomalies and temporal trends: data filtering**

498 The magnitude of CTI anomalies from long-term means in 2° × 2° grid cells shows the effect of
499 sampling effort on the uncertainty in these estimates (Supplementary Fig. 11a, b). As expected, given
500 the standard error of the mean being proportional to the underlying standard deviation multiplied by the
501 square root of the sample size, the magnitude of anomalies declined with the number of species records
502 (STIs) used to compute each CTI value (Supplementary Fig. 11a). CTI anomalies were omitted from
503 trend analysis for bottom-trawl surveys if comprising fewer than 20 species records. Similarly, annual
504 CTI anomalies tended to be larger when composed of fewer bottom trawls or plankton samples.
505 Estimates based on fewer than 10 bottom trawls or plankton hauls per year were also excluded from
506 further analysis (Supplementary Fig. 11b).

Standard errors associated with trends in CTI over time in each 2° × 2° grid cell were also related to the number of years sampled and the total species records over the time series in each cell (Supplementary Fig. 11c, d). Trends based on fewer than 10 years of data and less than 1000 species records were omitted from further analysis.

Analysis of trends in CTI versus community thermal traits: community thermal diversity (CTDiv), average thermal range width (CTR) and thermal bias, and predictions of sensitivity from simulated communities.

Relationships between trends in Community Temperature Index (as bootstrap-mean CTI_{SST}) and trends in sea temperature (HadISST), as modified by community thermal affinities, were analyzed by fitting least-squares multiple linear regression models (Supplementary Table 4). The relative importance of models was evaluated using Akaike weights. Intercepts were omitted from models because no CTI change would be expected where the temperature trend was zero (unless there was some delayed shift from an earlier period of warming or cooling). Adding intercepts back into these models (Models A and Ci to Ni) had very little effect on model fits (as shown by ΔAICc) or the parameter value estimates, and did not result in intercepts that were significantly different from zero.

Terms were introduced first as linear effects and then as squared terms, reflecting the results from the simulation model (Model Z). Modifying effects of average community thermal metrics (CTDiv, CTR, Thermal bias) and local vertical and horizontal gradients in average temperature were expressed as interactions with the temporal trend in sea surface temperature to address sensitivity of CTI to temperature. Considering effects only as interaction terms reflected the assumption that change in average thermal affinity would respond to changes in temperature, and that patterns of local average thermal diversity, species range, or thermal bias would modify that change in CTI in response to temperature. The model with the squared ratio of community thermal diversity (CTDiv) to species

530 thermal range (CTR, Model G) links the observational data with the simulation analysis. In simulations
531 using the Gaussian function, regression of log CTI sensitivity on log STR (=CTR in this case, since all
532 species in the simulation had the same STR) and CTDiv gave a perfect fit with coefficients of -2 and 2
533 respectively, which back transforms from logs to the one-parameter equation involving the squared
534 ratio of CTDiv to CTR (Model Z).

535 Adding the interactive effect of thermal diversity (CTDiv) to SST trend (dSST) produced a better
536 model (Model D vs B, $AICc_D$ - $AICc_B$ = -63.90), while adding thermal range (CTR) alone did not
537 (Model C vs B, $AICc_C$ - $AICc_B$ = -2.52). Including both factors, either as linear predictors (E) or
538 squared terms (F), further improved the model (Model E vs B, $AICc_E$ - $AICc_B$ = -82.62; Model F vs B,
539 $AICc_F$ - $AICc_B$ = -77.03). Thermal diversity was negatively correlated with inverse thermal range
540 width, resulting in large changes in parameter values when each factor was added to a model
541 containing the other. The squared-ratio model ($CTDiv^2$:CTR^2), Model G, equivalent to the model fitted
542 to simulation data (Z), had similar explanatory power to other models including those terms (E, F). The
543 parameter value for this model (G, 7.63) was close to the 6.54 obtained for simulated communities (Z).

544 Thermal bias affected CTI sensitivity in the simulations, negatively or positively depending on the
545 direction of skew of the abundance-temperature relationship, and so was introduced as an addition to
546 the squared ratio model. Adding thermal bias slightly improved model fit (Model H vs G, $AICc_H$ -
547 $AICc_G$ = -1.18) and increased the sensitivity of CTI by 0.04 for each °C of thermal bias. This positive
548 effect meant that communities comprising warm-water species showed greater change in CTI than
549 those composed of cold-water species for the same change in temperature. The effect was also
550 consistent with the effect of realized right-skewed (gamma) abundance-temperature distribution in the
551 simulations, but not a left-skewed one as implied by typical physiological thermal performance
552 curves[35].

553 Both horizontal and vertical gradients in temperature were expected to influence CTI sensitivity.
554 Steep vertical gradients in temperature may have a negative effect on CTI sensitivity because species
555 may be able to shift to cooler temperatures in the same area by moving deeper. Gentle horizontal
556 gradients in temperature, combined with temperature change through time, result in higher velocities of
557 climate and thereby more rapid distribution shifts among species[2, 18]. With a greater rate of species
558 turnover in areas of high climate velocity, we expected a negative relationship between CTI sensitivity
559 and the magnitude of the horizontal gradient in temperature. Adding shallow vertical temperature
560 differences (surface less 50m) improved the model with community thermal diversity and thermal
561 range (Model I vs G, $AICc_I$ - $AICc_G$ = -33.39), albeit with no effect of vertical differences from surface
562 to 100m (Model J) or 200m depth (Model K). Adding horizontal temperature gradient (Model L) to the
563 basic model (G) had a smaller effect on model fit ($AICc_L$ - $AICc_G$ = -3.15) and did show the expected
564 negative influence of the horizontal gradient. Combining vertical and horizontal gradients in
565 temperature (Model M) did not improve model fit, and the horizontal gradient coefficient did not differ
566 from zero. A regression model that included thermal bias effects as well as horizontal and vertical
567 gradients in temperature (Model N) was the most parsimonious, albeit with the parameter for horizontal
568 gradient not significantly different from zero. Residuals from the squared-ratio model proved to be
569 related most strongly to the effect of vertical temperature gradient (Model R1, Fig. 3b).

570 Cross validation of was used to examine the predictive skill of Model I (Supplementary Table 4,
571 Supplementary Fig. 12). We used dataset type (bottom trawls or plankton) and latitude and longitude
572 (giving contiguous spatial blocks) to split the data into near similar-sized training and test datasets, with
573 each set alternately used as the training set for the other test set of data. Choices of splits for latitude
574 (50°N) and longitude (40°W) were arbitrary, but adopted to produce adequately sized datasets for
575 fitting. Model I fitted to the plankton subset as training data (Model Icpr) and bottom-trawl subsets
576 (Model Idem) produced similar parameter estimates (significant $P<0.05$), with CTI trends for bottom

577 trawls explained markedly better. Splitting into plankton and demersal species gave the worst fits to the
578 other as test data (CV rsme 0.0284), the plankton training set predicting larger CTI trends than the
579 bottom-trawl training set. Splitting by latitude and longitude gave similar root mean squared errors to
580 the plankton / bottom-trawl split (Supplementary Table 4), but produced non-significant parameter
581 estimates for the vertical temperature gradient term for data west of 40°W. Model residuals for Model I
582 showed some spatial structure (Supplementary Fig. 12a), with evidence for spatial autocorrelation in
583 the CTI trends and in the predictor variables (Supplementary Fig. 12b-c).

584 Of all predictors tested beyond the effects of thermal diversity and thermal range, the vertical
585 temperature gradient effect had the largest influence on CTI sensitivity, (Fig. 3f). The apparent positive
586 effect of thermal bias was due to the negative association with vertical gradient for demersal species
587 (Fig. 3a), and the small negative effect of horizontal gradient was due to the weak positive association
588 of vertical and horizontal gradients of temperature, particularly in the northwest Atlantic.

589 **Evaluation of explanatory power of alternate sea temperature datasets in explaining spatial**
590 **variation in trends in CTI anomalies**

591 We fitted a subset of regression models in Supplementary Table 4 to every combination of four
592 variants of CTI and temperature trends from nine dataset layers: five surface layers (EN4SST,
593 COBESST, ERSST, HadISST and OISST, Supplementary Fig. 13) and four subsurface layers
594 (EN4SBT, EN4 50m depth, EN4 100m depth and EN4 200m depth). Models were fitted for every
595 bootstrap selection of species (n=500), with model fits and 95% bootstrap confidence intervals shown
596 in Supplementary Fig. 14. The most variation in CTI was explained for CTI_{SST} from STIs obtained by
597 matching modelled species distributions to surface temperature (aCTIen4sst and aCTIhadsst1), with the
598 poorest performance of models fitted to CTI_{SST} from STIs obtained by matching 1° mapped
599 observations of species presence in gridcells (from OBIS data summed for the period 1960 to 2009) to

surface temperatures (aCTIhadsst2). Trends in seabed temperatures did least well in terms of adjusted R^2 at predicting CTI_{SBT} or CTI_{SST}. Models that included terms for the squared ratio of thermal diversity to range width fitted better when in combination with magnitude of vertical gradient and/or horizontal gradient.

Data availability

The data that support the findings of this study are available at the publicly accessible repositories listed in Supplementary Table 1.The Community Temperature Index (CTI) values and species thermal affinity data that support the findings of this study are available as annual values and 30 year means[36] (Supplementary Fig. 7) and as trends[37] in 2° × 2° grid cells (Figs 2, 3, Supplementary Fig. 5). Species thermal affinities derived from models and observations are also available[38]. Source data for the analyses presented are available at links given in the supplementary information files. Source code for the simulation of CTI response to temperature change is available at https://github.com/michaeltburrows/ctisimulation (Fig. 1).

33. Kramer‐Schadt S, Niedballa J, Pilgrim JD, Schröder B, Lindenborn J, Reinfelder V, *et al.* The importance of correcting for sampling bias in MaxEnt species distribution models. *Divers Distrib* 2013, **19**(11)**:** 1366-1379.
34. Rodríguez-Sánchez F, De Frenne P, Hampe A. Uncertainty in thermal tolerances and climatic debt. *Nature Climate Change* 2012, **2**(9)**:** 636-637.
35. Dell AI, Pawar S, Savage VM. Systematic variation in the temperature dependence of physiological and ecological traits. *Proceedings of the National Academy of Sciences* 2011, **108**(26)**:** 10591-10596.
36. Burrows MT. Community Temperature Index values for North Pacific and North Atlantic bottom trawls and plankton in 2° latitude/longitude areas annually from 1985 to 2014, 2019. (https://doi.org/10.6084/m9.figshare.9699068).
37. Burrows MT. Trends in Community Temperature Index values for North Pacific and North Atlantic bottom trawl and plankton surveys for 2° latitude/longitude boxes from 1985 to 2014, 2019. (https://doi.org/10.6084/m9.figshare.9699107).
38. Burrows MT, Payne BL. Species Temperature Index and thermal range information forNorth Pacific and North Atlantic plankton and bottom trawl species, 2018. (https://doi.org/10.6084/m9.figshare.6855203.v1).
39 Brodie, B., Mowbray, F. & Power, D. *OBIS Canada Digital Collections*. http://www.obis.org/ (Bedford Institute of Oceanography, Dartmouth, NS, Canada, 2013).

40 DFO. *OBIS Canada Digital Collections*. http://www.obis.org/ (Bedford Institute of Oceanography, Dartmouth, NS, Canada, 2016).
41 Heessen, H. J., Daan, N. & Ellis, J. R. *Fish Atlas of the Celtic Sea, North Sea, and Baltic Sea: Based on International Research-vessel Surveys*. (Wageningen Academic Publishers, 2015).
42 ICES. https://datras.ices.dk/Data_products/Download/Download_Data_public.aspx (ICES, Copenhagen, Denmark, 2015).
43 Reid, P. C., Colebrook, J. M., Matthews, J. B. L., Aiken, J. & Team, C. P. R. The Continuous Plankton Recorder: concepts and history, from plankton indicator to undulating recorders. *Progress in Oceanography* **58**, 117 (2003).
44 Hirahara, S., Ishii, M. & Fukuda, Y. Centennial-Scale Sea Surface Temperature Analysis and Its Uncertainty. *J. Clim.* **27**, 57-75, doi:10.1175/jcli-d-12-00837.1 (2014).
45 Huang, B. *et al.* Extended reconstructed sea surface temperature, version 5 (ERSSTv5): upgrades, validations, and intercomparisons. *J. Clim.* **30**, 8179-8205 (2017).
46 Burnham, K. P. & Anderson, D. R. *Model Selection and Multimodel Inference: A Practical Information Theoretic Approach*. 2nd edn, (Springer Verlag, 2002).

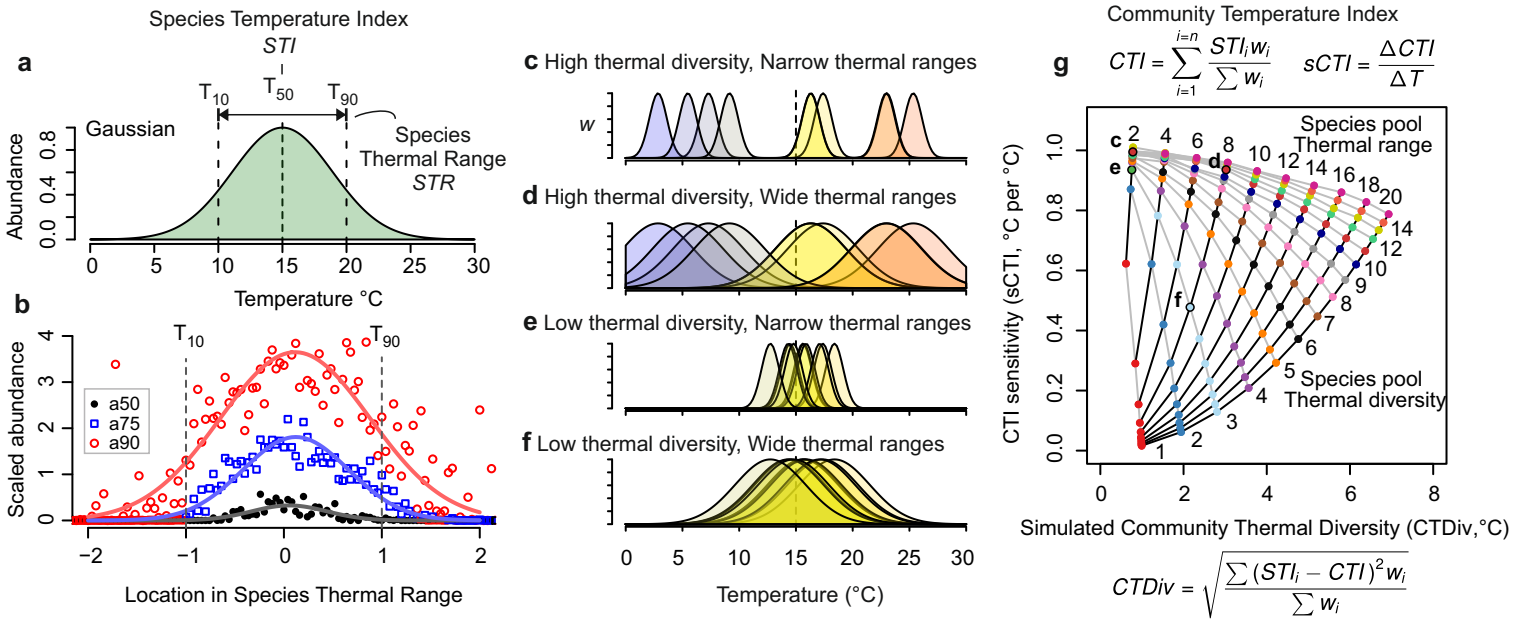
Species Temperature Index
STI
a
T10
T50
T90
Gaussian
Species
Thermal Range
STR
Abundance
0.0 0.4 0.8
0 5 10 15 20 25 30
Temperature °C
b
T10
T90
a50
a75
a90
Scaled abundance
0 1 2 3 4
−2 −1 0 1 2
Location in Species Thermal Range
c High thermal diversity, Narrow thermal ranges
w
d High thermal diversity, Wide thermal ranges
e Low thermal diversity, Narrow thermal ranges
f Low thermal diversity, Wide thermal ranges
0 5 10 15 20 25 30
Temperature (°C)
Community Temperature Index
g
$CTI = \sum_{i=1}^{i=n} \frac{STI_i w_i}{\sum w_i}$
$sCTI = \frac{\Delta CTI}{\Delta T}$
Species pool
Thermal range
Species pool
Thermal diversity
CTI sensitivity (sCTI, °C per °C)
0.0 0.2 0.4 0.6 0.8 1.0
0 2 4 6 8
Simulated Community Thermal Diversity (CTDiv,°C)
$CTDiv = \sqrt{\frac{\sum (STI_i - CTI)^2 w_i}{\sum w_i}}$

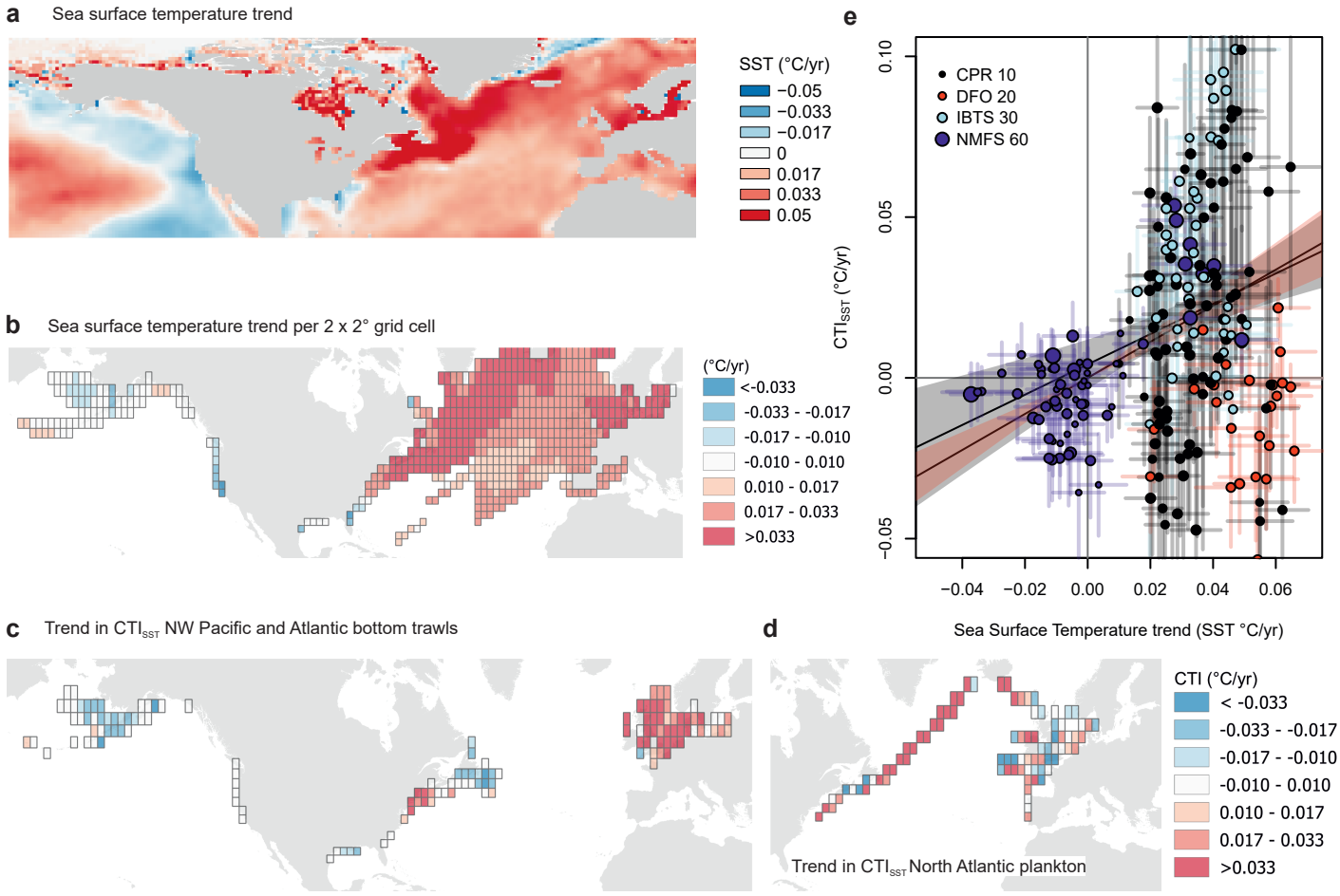
a
Sea surface temperature trend
SST (°C/yr)
−0.05
−0.033
−0.017
0
0.017
0.033
0.05
b
Sea surface temperature trend per 2 x 2° grid cell
(°C/yr)
<-0.033
-0.033 - -0.017
-0.017 - -0.010
-0.010 - 0.010
0.010 - 0.017
0.017 - 0.033
>0.033
e
CPR 10
DFO 20
IBTS 30
NMFS 60
CTI$_{SST}$ (°C/yr)
0.10
0.05
0.00
−0.05
−0.04
−0.02
0.00
0.02
0.04
0.06
Sea Surface Temperature trend (SST °C/yr)
c
Trend in CTI$_{SST}$ NW Pacific and Atlantic bottom trawls
d
Trend in CTI$_{SST}$ North Atlantic plankton
CTI (°C/yr)
< -0.033
-0.033 - -0.017
-0.017 - -0.010
-0.010 - 0.010
0.010 - 0.017
0.017 - 0.033
>0.033

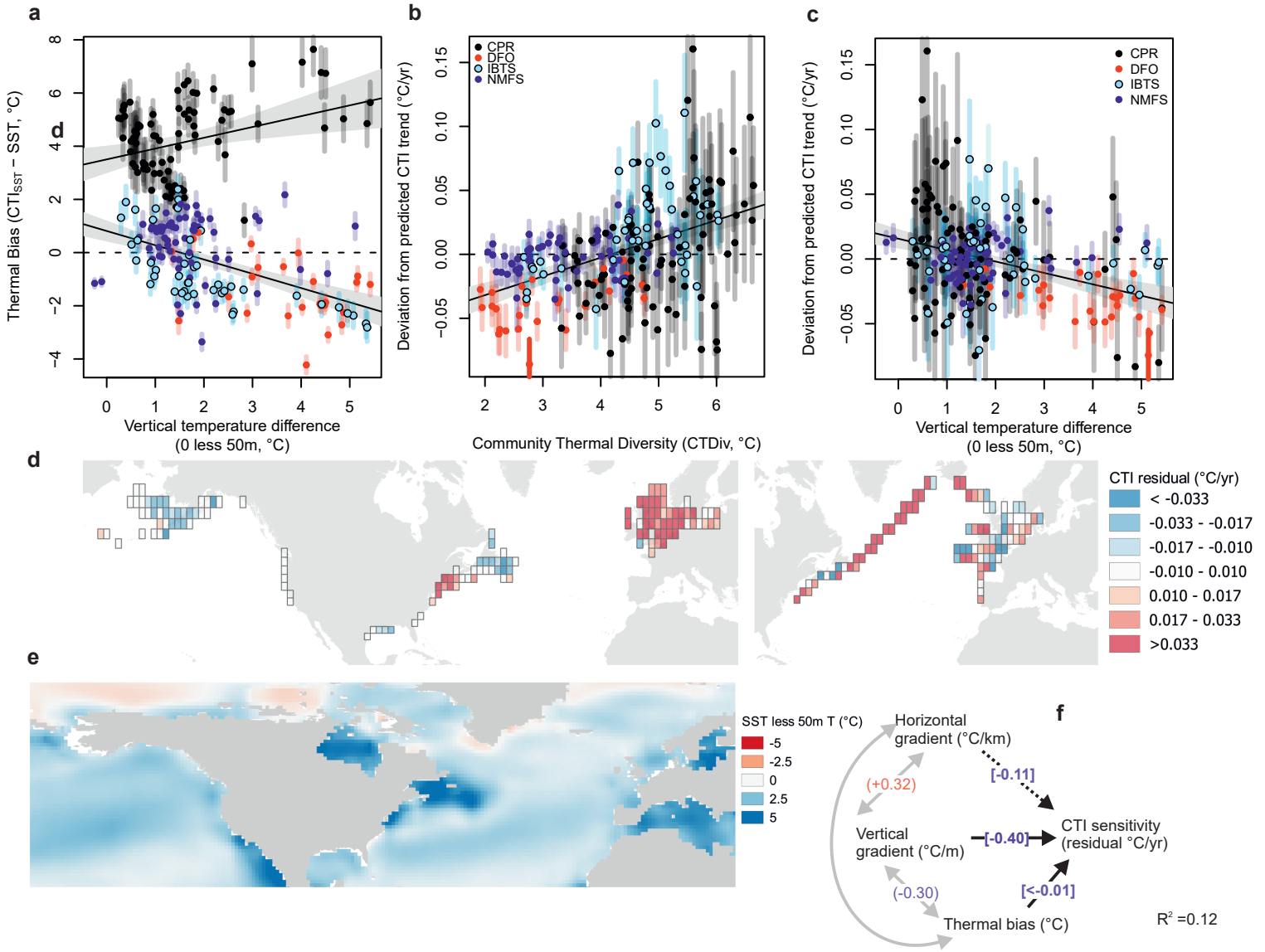
a
b
c
d
e
f
Thermal Bias (CTI$_{SST}$ − SST, °C)
Vertical temperature difference (0 less 50m, °C)
Deviation from predicted CTI trend (°C/yr)
Community Thermal Diversity (CTDiv, °C)
CPR
DFO
IBTS
NMFS
CTI residual (°C/yr)
< -0.033
-0.033 - -0.017
-0.017 - -0.010
-0.010 - 0.010
0.010 - 0.017
0.017 - 0.033
>0.033
SST less 50m T (°C)
-5
-2.5
0
2.5
5
Horizontal gradient (°C/km)
Vertical gradient (°C/m)
Thermal bias (°C)
CTI sensitivity (residual °C/yr)
(+0.32)
[-0.11]
[-0.40]
(-0.30)
[<-0.01]
R^2 =0.12